CrossMark

^{1}H MRS spectroscopy in preclinical autosomal dominant Alzheimer disease

Elizabeth Joe[1] · Luis D. Medina[2,3] · John M. Ringman[1,2] · Joseph O'Neill[4]

Abstract

^{1}H magnetic resonance spectroscopy (MRS) can reveal changes in brain biochemistry in vivo in humans and has been applied to late onset Alzheimer disease (AD). Carriers of mutations for autosomal dominant Alzheimer disease (ADAD) may show changes in levels of metabolites prior to the onset of clinical symptoms. Proton MR spectra were acquired at 1.5 T for 16 cognitively asymptomatic or mildly symptomatic mutation carriers (CDR < 1) and 11 non-carriers as part of a comprehensive cross-sectional study of preclinical ADAD. Levels of N-acetyl-aspartate+N-acetyl-aspartyl-glutamate (NAA), glutamate/glutamine (Glx), creatine/phosphocreate (Cr), choline (Cho), and *myo*-inositol (mI) in the left and right anterior cingulate and midline posterior cingulate and precuneus were compared between mutation carriers (MCs) and non-carriers (NCs) using multivariate analysis of variance with age as a covariate. Among MCs, correlations between metabolite levels and time until expected age of dementia diagnosis were calculated. MCs had significantly lower levels of NAA and Glx in the left pregenual anterior cingulate cortex, and lower levels of NAA and higher levels of mI and Cho in the precuneus compared to NCs. Increased levels of mI were seen in these regions in association with increased proximity to expected age of dementia onset. MRS shows effects of ADAD similar to those seen in late onset AD even during the preclinical period including lower levels of NAA and higher levels of mI. These indices of neuronal and glial dysfunction might serve as surrogate outcome measures in prevention studies of putative disease-modifying agents.

Keywords Autosomal dominant Alzheimer disease · Magnetic resonance spectroscopy · Presymptomatic · Biomarker

Introduction

The neurodegenerative processes characteristic of Alzheimer disease (AD) predate the development of clinical dementia by decades (Bateman et al. 2012; Katzman et al. 1988). These changes include neuronal loss and the development of amyloid plaques, neurofibrillary tangles and associated gliosis (Scheltens et al. 2016). Persons in this presymptomatic stage provide the opportunity to prevent the symptomatic disease and the development of therapeutics that target this early neurodegeneration requires biomarkers that accurately predict the development and progression of clinical dementia. A number of biomarkers have been proposed to behave in a predictable fashion in AD including beta-amyloid (Aβ) peptide and hyperphosphorylated tau protein levels in the cerebrospinal fluid (CSF), a specific pattern of hypometabolism on FDG-PET, identification of amyloid pathology using amyloid PET and hippocampal atrophy on structural MRI (Jack et al. 2010, 2011, 2013). These biomarker changes have also been identified in ADAD (Bateman et al. 2012; Ringman et al. 2008). These biomarkers, however, have limitations including accessibility in clinical practice, standardization, and the definition of cut-off thresholds for reliable identification of AD pathology.

^{1}H magnetic resonance spectroscopy (MRS) provides a way to study brain biochemical processes in vivo. In patients

✉ Elizabeth Joe
  elizabeth.joe@med.usc.edu

1   Alzheimer Disease Research Center, Keck School of Medicine, Univeristy of Southern California, Center for Health Professions, 1540 Alcazar Street, Los Angeles, CA 90033, USA

2   Easton Center for Alzheimer's Disease Research, University of California, Los Angeles, 710 Westwood Plaza, Room C-224, Los Angeles, CA 90095, USA

3   Department of Neurosurgery, University of Colorado School of Medicine, 12631 E. 17th Ave., C307, Aurora, CO 80045, USA

4   Division of Child & Adolescent Psychiatry, Semel Institute For Neuroscience, University of California, Los Angeles, 760 Westwood Plaza, 58-227, Los Angeles, CA 90095, USA

⚠ Springer

with dementia due to AD, ^{1}H MRS has consistently shown decreases in *N*-acetylaspartate (NAA), which is produced in neuronal mitochondria and found predominantly in neurons, as well as increased levels of myo-inositol (mI), a glial cell marker (Wang et al. 2015; Zhang et al. 2014). Alterations in the levels of these metabolites have been shown to correlate with the neuropathological findings in AD (Kejal Kantarci et al. 2008; Murray et al. 2014) and to also correlate with performance on tests of cognition (Frederick et al. 2004). Changes in NAA/Cr in the occipital cortex (Modrego et al. 2005, 2011), posteromedial parietal lobe (including the posterior cingulate gyrus and precuneus) (Modrego et al. 2011), and left paratrigonal white matter (Metastasio et al. 2006) as well as mI/Cr in the right parietal lobe (Targosz-gajniak et al. 2013) also appear to predict cognitive decline and conversion to dementia in patients with amnestic mild cognitive impairment (MCI). Results of ^{1}H MRS studies of other metabolites including Cho (representing phosphatidyl choline and other membrane precursors, a marker of membrane turnover), Cr (representing creatine and phosphocreatine) and Glx (representing glutamate and glutamine) have been less consistent (Zhang et al. 2014). Prior ^{1}H MRS studies in AD have been limited in the preclinical stage of the disease due to the difficulty of identifying appropriate subjects.

Autosomal dominant AD is caused by mutations in the *PSEN1*, *APP*, and *PSEN2* genes with symptoms typically starting at a relatively young age. This population represents an opportunity to study metabolite levels in preclinical AD since carriers of the mutation develop AD with essentially 100% penetrance. A single study of 7 such ADAD mutation carriers (MCs) previously showed lower ratios of NAA/Cr and NAA/mI compared to non-carriers (NCs) in a single midline voxel containing the posterior cingulate (Godbolt et al. 2006). In the present study we attempted to identify if these changes are seen more broadly and at what stage in ADAD.

Methods

Subjects were participants in a comprehensive study of preclinical and manifest ADAD at a tertiary dementia referral center. The study was approved by the University of California, Los Angeles (UCLA) Human Subjects Committee and informed consent was obtained from all individual participants included in the study. All subjects were first-degree relatives of someone known to carry a pathogenic mutation in the *PSEN1*, *APP*, or *PSEN2* genes, placing them at 50% risk for inheriting such a mutation and therefore developing ADAD. Genetic testing for the relevant mutation was performed as part of this study but subjects were not informed of the results. Revealing clinical genetic testing was offered outside of the research protocol for interested subjects. Extraction of DNA and genotyping of apolipoprotein E
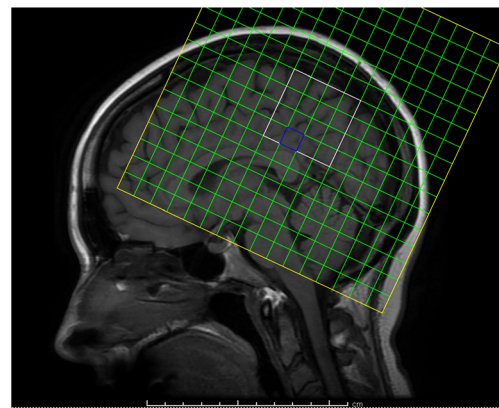
Fig. 1 Sagittal T1-weighted MRI of the human brain showing prescription of midline parietal ^{1}H MRSI slab (yellow box). Usable spectra are obtained from the voxels (green squares) within the PRESS excitation volume (white box)

(*APOE*) were performed using standard techniques. *APOE* SNP genotyping was carried out by real-time PCR on an Applied Biosystems 7900HT Real Time PCR machine (Applied Biosystems, Foster City, CA), using Taqman SNP Genotyping Assays (#C3084793_20 and C904973_10 for rs429358 and rs7412, respectively). The SDS version 2.3 software was used to analyze the raw data and to call the genotype. The presence or absence of the specific mutation each subject was known to be at-risk for were assessed using standard Sanger sequencing, according to published protocols and primers.

The Clinical Dementia Rating Scale (CDR) was performed with an unrelated informant (Morris 1997). The CDR is a structured interview with input from both the subject and an informant who knows the subject well. In the CDR,
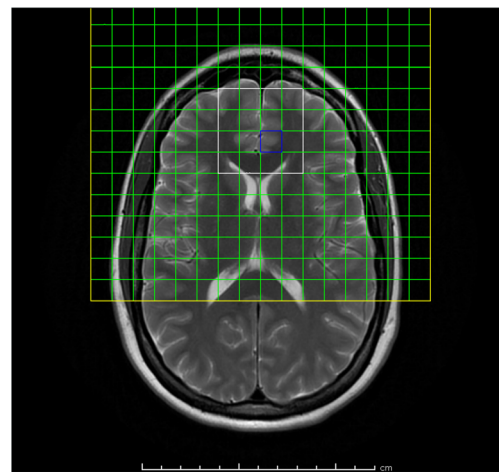
Fig. 2 T2-weighted axial-oblique (parallel to genu-splenium line) MRI of the human brain showing prescription of anterior cingulate ^{1}H MRSI slab (yellow box). Usable spectra are obtained from the voxels (green squares) within the PRESS excitation volume (white box). Posterior mesial voxels within the slab sample left and right pregenual anterior cingulate cortex (LpAC, RpAC), anterior mesial voxels sample mesial superior frontal cortex, lateral voxels sample prefrontal white matter (anterior corona radiata)

Table 1 Patient characteristics

	MC (*n* = 16)	NC (*n* = 11)
Female gender (%)	13 (81%)	8 (73%)
Mean age (s.d.)	**32.6 (7.0)**	**40.1* (10.0)**
Mean years until median age of dementia onset in the family (s.d.)	12.3 (8.7)	4.64 (13.4)
Family mutation (%)		
PSEN1	13 (81%, 11 A431E, 2 L235 V)	8 (80%, 7 A431E, 2 L235 V)
APP	3 (19%, V717I)	2 (20%, V717I)
APOE genotype (%)		
3/3	11 (69%)	8 (73%)
3/4	2 (13%)	2 (18%)
2/3	3 (19%)	1 (9%)
CDR = 0	11 (69%)	9 (82%)
CDR = 0.5	5 (31%)	2 (18%)

Bold indicates a statistically significant difference between MC and NC

*$p = 0.03$

asymptomatic persons are rated 0, and persons with questionable cognitive impairment are rated 0.5. Scores of 1, 2, and 3 represent mild, moderate, and severe stages of dementia, respectively. Subjects with clinical dementia (CDR of 1 or higher) were excluded from the analysis.

Each subject's age in relation to their estimated age of dementia diagnosis was calculated. As the age of onset of symptoms is fairly consistent within a family and mutation but more variable between families (Ryman et al. 2014), an "adjusted age" can be calculated that estimates how many years from disease manifestation a given subject is (Ryman et al. 2014). In our experience, we have found that the age of clinical diagnosis of dementia is a more reproducible measure and therefore we calculated an adjusted age for each subject as his or her chronological age minus the median age of dementia diagnosis in his or her family.

Whole-brain structural MRI and water-suppressed ^{1}H MRS were acquired at 1.5 T on a Siemens Sonata scanner. MRS was acquired in 2D magnetic resonance spectroscopic imaging (MRSI) configuration with a point-resolved spectroscopy sequence (PRESS) with repetition-time (TR) of 1500 ms, echo-time (TE) of 30 ms, and 8 excitations. Two 4×4 MRSI arrays or "slabs" (i.e., PRESS excitation volumes within 16×16 phase-encoding grids) were acquired, each with in-plane voxel resolution of 11×11 mm^2. The first slab[16] was 9 mm thick and axial-oblique, oriented parallel to the genu-splenium plane. It was positioned dorsoventrally symmetrically about the genu of the corpus callosum and left-right symmetrically astride the longitudinal fissure with the

Table 2 Results of multivariate analysis of covariance by voxel

Voxel	F	*p*
LpAC	**3.067**	**0.040**
RpAC	0.761	0.592
mPCG	1.461	0.264
mPC	**4.400**	**0.013**

Bold numbers indicate statistically significant findings

LpAC left pregenual anterior cingulate gyrus, *RpAC* right pregenual anterior cingulate gyrus, *mPCG* midline posterior cingulate gyrus, *mPC* midline precuneus

Table 3 ^{1}H-MRS mean metabolite values by voxel in MCs and NCs

| Voxel	Metabolite	MC Mean	MC SD	NC Mean	NC SD	*p*
LpAC	Cho	1.66	0.21	1.84	0.34	0.174
	Cr	5.13	0.50	5.37	1.12	0.480
	mI	4.63	0.66	4.72	0.89	0.802
	NAA	**7.62**	**0.42**	**8.38**	**1.32**	**0.046***
	Glx	**12.84**	**1.99**	**13.55**	**2.53**	**0.007***
RpAC	Cho	1.66	0.34	1.75	0.20	0.833
	Cr	5.71	0.91	5.59	1.28	0.632
	mI	5.04	0.81	5.04	1.04	0.846
	NAA	7.84	0.95	8.37	0.75	0.336
	Glx	14.54	2.66	13.37	1.31	0.183
mPCG	Cho	1.63	0.24	1.65	0.07	0.439
	Cr	6.76	1.22	6.82	0.99	0.698
	mI	5.86	1.36	5.33	0.62	0.055
	NAA	9.48	0.77	9.83	1.06	0.366
	Glx	12.50	1.44	13.08	2.36	0.190
mPC	Cho	**1.24**	**0.15**	**1.20**	**0.13**	**0.032***
	Cr	6.09	0.45	6.30	0.75	0.757
	mI	**5.34**	**0.97**	**4.27**	**0.55**	**0.0004***
	NAA	**8.87**	**0.38**	**9.66**	**0.81**	**0.036***
	Glx	14.10	1.09	14.12	1.58	0.867

Bold numbers indicate statistically significant findings

LpAC left pregenual anterior cingulate gyrus, *RpAC* right pregenual anterior cingulate gyrus, *mPCG* midline posterior cingulate gyrus, *mPC* midline precuneus

*significant protected post-hoc ANCOVA

posterior slab edge abutting the genual rostrum. Posterior voxels within the slab sampled left and right pregenual anterior cingulate cortex (LpAC and RpAC, respectively) (Fig. 1). The second slab (O'Neill et al. 2015) was 12 mm thick and sagitally oriented. It was positioned left-right symmetrically astride the longitudinal fissure. The rear edge of the slab was aligned parallel to the parieto-occipital sulcus; the inferior edge was parallel or tangent to the dorsal margin of the isthmus or splenium of the corpus callosum. Thus, the slab sampled midline posterior cingulate (mPCG; inferior voxels) and midline precuneus (mPC; superior voxels) (Fig. 2). MR spectra were fit automatically with the LCModel commercial software package (Provencher 2001) yielding levels of NAA, Glx, Cr, Cho, and mI, referenced to unsuppressed water and expressed in institutional units (IU). Water-reference was

preferred to referencing metabolite ratios to Cr due to certain weaknesses of the latter (Alger 2011). Cr measurement can be limited by overlap with neighboring signals (especially Cho). The Cr signal is a much smaller than the water signal and is thus more sensitive to noise. Also, accumulating evidence that Cr varies across the brain, with age, and with disease has gradually undermined earlier faith in Cr as a constant standard. After segregation of the whole brain MRI into gray matter, white matter, and CSF binary masks (Shattuck et al. 2001) the MRSI Voxel Picker (MVP) package (Seese et al. 2011) was used to compute the volume percent of gray matter, white matter, and CSF in each voxel and correct the LCModel-derived levels of each metabolite for voxel CSF content. Spectra not meeting quality control criteria (linewidth ≤ 0.1 ppm and signal-to-noise ratio ≥ 3) were rejected.
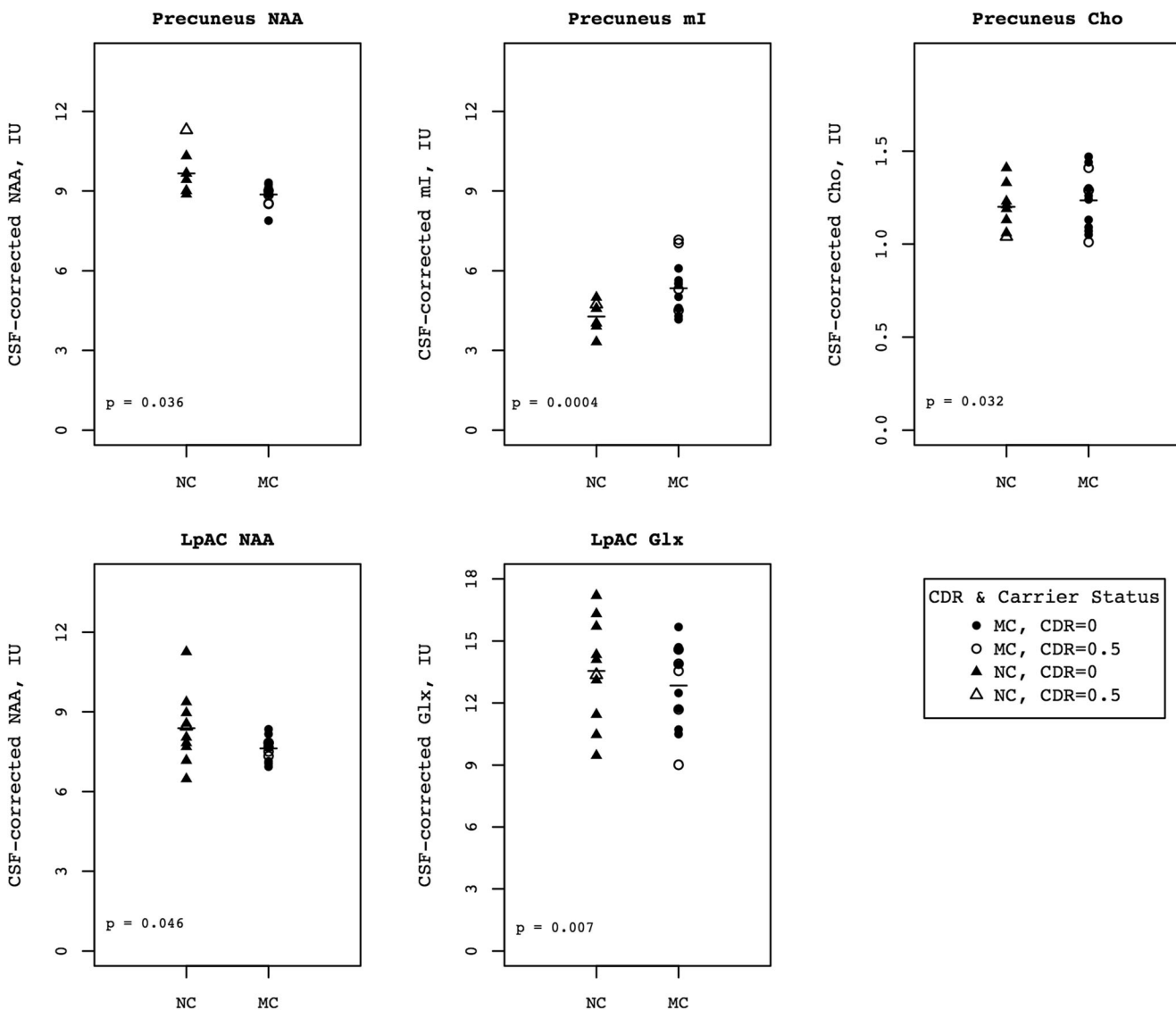
Fig. 3 Metabolite levels by carrier status and CDR for voxels/metabolite combinations for which there was a significant effect by carrier status. Horizontal bars represent mean metabolite values for the entire group (including individuals with both CDR 0 and 0.5)

Additionally, within spectra, individual metabolite peaks were rejected that were not considered reliable by LCModel (standard deviation of metabolite signal >20%).

Characteristics of the study population were compared using two-sided Fisher exact tests for nominal variables and Student's t-test for quantitative variables. For comparison between groups and regions of interest, a multivariate analysis of covariance (MANCOVA) with age as a covariate was performed for each region of interest across five metabolites (NAA, Glx, Cr, Cho, and mI). If the overall MANCOVA for a region showed a significant effect of diagnosis, protected post-hoc ANCOVA testing was performed for individual metabolites.

Within the MC group, we determined whether there was a correlation between metabolite levels and time until expected onset of dementia using a Spearman correlation. To correct for multiple comparisons a Holm-Bonferroni test was applied. A p value <0.05 was considered statistically significant. All statistical analyses were conducted in R version 3.3.1.

Results

The study population was comprised of 16 preclinical (CDR < 1) MCs and 11 NC controls with MRS data acquisition as part of the above study protocol. Data were missing from 3 MCs for the LpAC and RpAC, and 3 different MCs for mPCG and mPC; data were missing from 1 NC for LpAC, 2 NCs for RpAC, and 3 NCs for mPCG and mPC. These subjects were excluded from the analysis of the relevant voxels. Demographic information for the study participants is found in Table 1. The majority of MCs carried a mutation in *PSEN1* (n = 13) while the remaining 3 had mutations in *APP*. Among MCs, 11 had CDR of 0 and 5 had CDR of 0.5. Among NCs, 2 subjects were blindly rated as having a CDR score of 0.5 but considering their ages (37 and 39), the etiology was considered unlikely to represent early AD. There was a significant difference in mean age between MCs (33, range 19–43) and NCs (40, range 28–59) (p = 0.03). Study participants were predominantly female (81 and 73% in MCs and NCs, respectively; not significant). Most participants were APOE $\varepsilon3/\varepsilon3$ or $\varepsilon2/\varepsilon3$ genotype, with 2 in each group being $\varepsilon3/\varepsilon4$ (13 and 18%, respectively; not significant). The mean time until expected onset of dementia in MCs was 12.3 years.

Results of MANCOVA analysis for the five metabolites of interest by voxel with age as a covariate showed a significant effect of mutation status in the LpAC (F = 3.067, p = 0.040) and mPC (F = 4.400, p = 0.013) (Tables 2 and 3). There was no effect of diagnosis in the RpAC or mPCG. Post-hoc protected ANCOVA with age as a covariate in the LpAC showed that MCs had lower NAA than NCs (7.61 vs 8.38, p = 0.04) and lower Glx (12.84 vs 13.55, p = 0.007). In the mPC, MCs had higher mI compared to NCs (5.3 vs 4.2, p =

0.0004), higher Cho (1.23 vs 1.20, p = 0.03) and lower NAA (8.86 vs 9.66, p = 0.04) (Fig. 3).

Metabolite levels for MCs and NCs are listed in Table 3; while we did not use Cr-normalized values for this analysis, we do report them for reference in Tables 4. Among MCs, the level of mI in the LpAC (ρ = −0.88, p = 0.00007) and mPC (ρ = −0.84, p = 0.0003) was higher in subjects with age closer to the estimated age of dementia diagnosis (Fig. 4, Table 5). Levels of Cr, Cho and mI all increased in the mPCG as onset of dementia approached, as did levels of Glx in the mPC however these findings did not remain significant after correcting for multiple comparisons. There were no other significant correlations between metabolite levels and time until expected onset of dementia in MCs (Table 5).

Discussion

In this study we found that preclinical ADAD MCs had higher levels of mI in the mPC than NCs, and that levels of mI in the mPC as well as the LpAC increased in association with progressive neurodegeneration. mI levels have been consistently shown to be above-normal in ^{1}H MRS studies of AD and elevated levels of mI appear to predate the development of dementia or alterations in other metabolites (K. Kantarci et al. 2000). The mean time until expected onset of dementia

Table 4 Cr-normalized ^{1}H-MRS mean metabolite values by voxel in MCs and NCs

Voxel	Metabolite	MC Mean	MC SD	NC Mean	NC SD
LpAC	Cho/Cr	0.33	0.05	0.36	0.10
	mI/Cr	0.91	0.13	0.90	0.16
	NAA/Cr	1.51	0.13	1.60	0.28
	Glx/Cr	2.58	0.45	2.65	0.79
RpAC	Cho/Cr	0.30	0.04	0.33	0.08
	mI/Cr	0.87	0.11	0.90	0.11
	NAA/Cr	1.41	0.23	1.55	0.24
	Glx/Cr	2.61	0.49	2.51	0.49
mPCG	Cho/Cr	0.25	0.06	0.25	0.03
	mI/Cr	0.88	0.16	0.79	0.05
	NAA/Cr	1.44	0.20	1.47	0.15
	Glx/Cr	1.91	0.33	1.94	0.26
mPC	Cho/Cr	0.20	0.02	0.19	0.03
	mI/Cr	0.88	0.14	0.67	0.05
	NAA/Cr	1.49	0.14	1.57	0.16
	Glx/Cr	2.38	0.15	2.29	0.27

LpAC left pregenual anterior cingulate gyrus, *RpAC* right pregenual anterior cingulate gyrus, *mPCG* midline posterior cingulate gyrus, *mPC* midline precuneus

Fig. 4 Correlation of PC and LpAC mI with years until expected diagnosis for MCs for asymptomatic (CDR = 0) and questionably symptomatic (CDR = 0.5) individuals
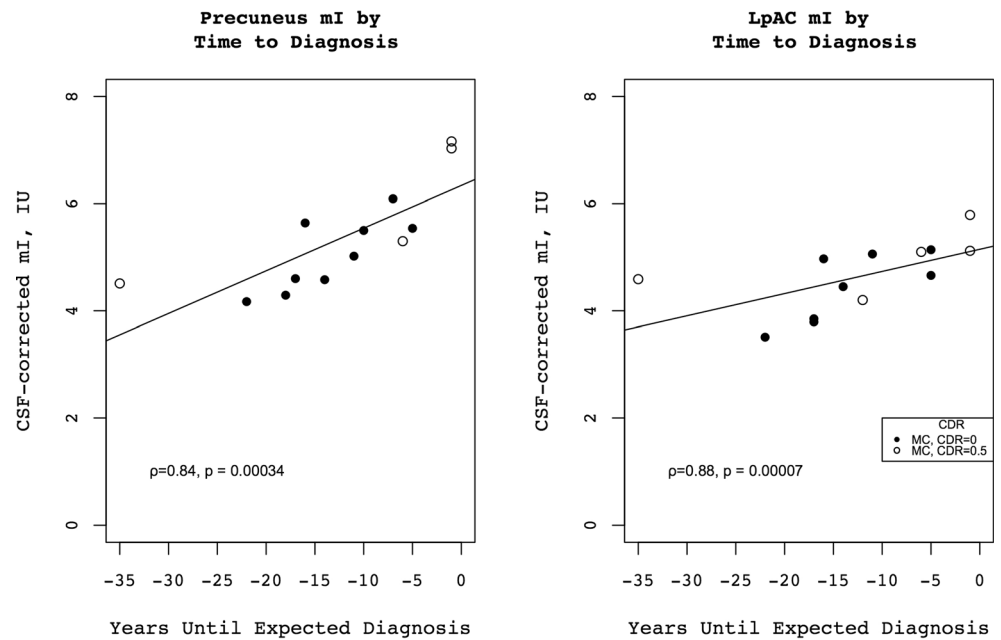
for MCs in this study was more than 12 years, confirming that mI is highly sensitive to early pathologic changes in AD.

mI is found primarily in glial cells, particularly astrocytes, where it appears to function as a cellular osmolyte and in cell signaling (Fisher et al. 2002). Elevated levels are thought to represent glial proliferation and/or greater cell size (Soares and Law 2009). In a postmortem study examining pathologic correlates of ^{1}H MRS metabolites in AD, mI/Cr has been shown to correlate with Aβ burden (Murray et al. 2014) rather than gliosis or neurofibrillary tangles. Since early pathologic changes in AD are predominantly related to amyloid deposition, this supports the role of mI as an early marker of AD pathology.

Studies of late-onset AD which have consistently shown diffusely below-normal levels of NAA (K. Kantarci et al. 2000; Zhang et al. 2014), and reductions in NAA/Cr levels have been shown to correlate with reduced synaptic integrity and increased hyperphosphorylated tau pathology (Murray et al. 2014). The NAA peak reflects mainly N-acetylaspartate with a smaller contribution from N-acetylaspartylglutamate (NAAG). NAA is synthesized by neuronal mitochondria and is predominantly found in neurons, although it is eventually transported out and degraded on the oligodendrocyte cell membrane; the exact function is unknown although it is thought to possibly represent an osmolyte (Hajek and Dezortova 2008; Soares and Law 2009). NAAG is synthesized from NAA and glutamate in neurons and appears to be involved in signaling local energy balance (Baslow 2016). Depressed levels of NAA are therefore thought to reflect either neuronal loss, impaired neuronal functioning or energy metabolism. We found that levels of NAA in the mPC and LpAC were lower in MCs than in NCs. The Glx peak, which represents glutamate and glutamine, has been shown to be below-normal in the anterior

Table 5 Correlation between metabolite levels and expected time to onset of AD

		Spearman ρ, years until expected diagnosis	p
LpAC	Cho	−0.29	0.344
	Cr	−0.37	0.212
	Gx	0.36	0.229
	mI	**−0.88**	**0.00007***
	NAA	−0.50	0.079
RpAC	Cho	−0.17	0.578
	Cr	−0.48	0.097
	Gx	−0.45	0.123
	mI	−0.45	0.123
	NAA	−0.01	0.969
mPCG	Cho	−0.76	0.003
	Cr	−0.68	0.010
	Gx	−0.26	0.388
	mI	−0.76	0.003
	NAA	−0.41	0.160
mPC	Cho	−0.52	0.072
	Cr	−0.46	0.117
	Gx	−0.66	0.015
	mI	**−0.84**	**0.00034***
	NAA	0.04	0.890

Bold numbers indicate statistically significant findings

LpAC left pregenal anterior cingulate gyrus, *RpAC* right pregenal anterior cingulate gyrus, *mPCG* midline posterior cingulate gyrus, *mPC* midline precuneus

*significant after Holm-Bonferroni correction for multiple comparisons

cingulate in AD (Huang et al. 2016); we also found MCs to have lower levels of Glx in the LpAC compared to NCs.

MCs also had elevated mPC Cho compared to NCs. The Cho peak includes phosphocholine and other precursors needed for synthesis of membranes; increased levels are thought to reflect membrane disruption, cellular proliferation or inflammation (Hajek and Dezortova 2008). Choline is also a precursor of the neurotransmitter acetylcholine, the deficit of which is an important part of the pathophysiology of AD. In late-onset AD, the role of Cho has been less clear with some studies supporting elevated levels in AD and others finding no effect (K. Kantarci et al. 2000; Wang et al. 2015); in addition, studies of neuropathological correlates of ^{1}H MRS metabolites in AD have not shown a clear correlation between Cho/Cr and AD pathology (Kejal Kantarci et al. 2008; Murray et al. 2014).

To our knowledge only one prior study has looked at ^{1}H MRS metabolites in ADAD. This single-voxel study examined metabolic changes in the posterior cingulate and found that presymptomatic MCs had depressed NAA/Cr and NAA/mI in the region of interest. In the present study, the mean level of mPCG NAA was lower in MCs but the difference was not statistically significant. This discrepancy may be partially explained by a longer time until expected diagnosis in our subjects (12.3 years vs 9.8); as mentioned above, NAA has been shown to correlate with hyperphosphorylated tau pathology and reduced synaptic integrity, which are thought to occur later in AD than amyloid deposition (Jack et al. 2010); thus it is possible that the difference between MCs and NCs would continue to diverge with time until the difference reached statistical significance. Other factors that may have contributed to our not fully replicating the previous finding include technical factors and choice of voxel placement. We did find that both mI and Cho in this region increased as age of expected diagnosis approached; although this finding was not significant after correction for multiple comparisons, it does suggest that this area is affected relatively early in the disease as is known from studies of late-onset AD.

Our study was limited by the relatively small number of subjects enrolled ($n = 27$). This is a common problem in studies of ADAD due to its relative rarity as a cause of AD. However, despite the small number of subjects we were able to show clear differences between MCs and NCs. MCs were also younger on average than NCs, likely in part because we excluded persons with clinical dementia, and the typical age of onset of clinical dementia in ADAD is frequently in the 5th decade. However since there is a decrease in NAA and increase in mI in normal aging (Minati et al. 2007) the increased age in NC controls would have acted to decrease between group differences, and thus would not impact the validity of our results. Finally, two NCs were blindly rated 0.5 on the CDR; given their young ages (37 and 39), the etiology was considered unlikely to represent early AD and more

likely due to heightened anxiety and potentially depression associated with living at-risk for ADAD. CDR rating is dependent on both the report of informants and subjects and anticipation of the onset of symptoms may have led them to emphasize subtle symptoms not related to incipient neurodegenerative disease.

In summary, levels of brain metabolites are altered in MCs for ADAD compared to NCs many years prior to expected onset of clinical dementia. mI is most sensitive as an early marker of AD pathology. For studies of disease-modifying interventions targeting prevention of neuronal death, MRS measures may provide an important surrogate outcome measure.

Compliance with ethical standards

Conflict of interest The authors declare that they have no conflict of interest.

Ethical approval All procedures performed in studies involving human participants were in accordance with the ethical standards of the institutional and/or national research committee and with the 1964 Helsinki declaration and its later amendments or comparable ethical standards. This article does not contain any studies with animals performed by any of the authors.

Informed consent Informed consent was obtained from all individual participants included in the study.

References

Alger, J. (2011). Quantitative proton magnetic resonance spectroscopy and spectroscopic imaging of the brain: a didactic review. *Topics in Magnetic Resonance Imaging, 21*(2), 115–128. https://doi.org/10.1097/RMR.0b013e31821e568f.Quantitative.

Baslow, M. H. (2016). An answer to "the nagging question of the function of N-Acetylaspartylglutamate". *Neuroscience Communications*, 2–7. https://doi.org/10.14800/nc.844.

Bateman, R. J., Xiong, C., Benzinger, T. L. S., Fagan, A. M., Goate, A., Fox, N. C., … & Dominantly Inherited Alzheimer Network. (2012). Clinical and biomarker changes in dominantly inherited Alzheimer's disease. *The New England Journal of Medicine, 367*(9), 795–804. https://doi.org/10.1056/NEJMoa1202753.

Fisher, S. K., Novak, J. E., & Agranoff, B. W. (2002). Inositol and higher inositol phosphates in neural tissues: homeostasis, metabolism and functional significance. *Journal of Neurochemistry, 82*(4), 736–754. https://doi.org/10.1046/j.1471-4159.2002.01041.x.

Frederick, B. D., Kyoon, I., Satlin, A., Heup, K., Kim, M. J., Yurgelun-todd, D. A., …, & Renshaw, P. F. (2004). In vivo proton magnetic resonance spectroscopy of the temporal lobe in Alzheimer's disease, 28, 1313–1322. https://doi.org/10.1016/j.pnpbp.2004.08.013.

Godbolt, A. K., Waldman, A. D., MacManus, D. G., Schott, J. M., Frost, C., Cipolotti, L., …, & Rossor, M. N. (2006). MRS shows abnormalities before symptoms in familial Alzheimer disease. *Neurology, 66*, 718–722. https://doi.org/10.1212/01.wnl.0000201237.05869.df.

Hajek, M., & Dezortova, M. (2008). Introduction to clinical in vivo MR spectroscopy. *European Journal of Radiology, 67*(2), 185–193. https://doi.org/10.1016/j.ejrad.2008.03.002.

Huang, D., Liu, D., Yin, J., Qian, T., Shrestha, S., & Ni, H. (2016). Glutamate-glutamine and GABA in brain of normal aged and patients with cognitive impairment. *European Radiology*, 1–7. https://doi.org/10.1007/s00330-016-4669-8.

Jack, C. R., Knopman, D. S., Jagust, W. J., Shaw, L. M., Aisen, P. S., Weiner, M. W., …, & Trojanowski, J. Q. (2010). Hypothetical model of dynamic biomarkers of the Alzheimer's pathological cascade. *Lancet Neurology, 9*(1), 119–128. https://doi.org/10.1016/S1474-4422(09)70299-6.

Jack, C. R., Vemuri, P., Wiste, H. J., Weigand, S. D., Aisen, P. S., Trojanowski, J. Q., …, & Alzheimer's Disease Neuroimaging Initiative. (2011). Evidence for ordering of Alzheimer disease biomarkers. *Archives of Neurology, 68*(12), 1526–35. https://doi.org/10.1001/archneurol.2011.183.

Jack, C. R., Knopman, D. S., Jagust, W. J., Petersen, R. C., Weiner, M. W., Aisen, P. S., …, & Trojanowski, J. Q. (2013). Tracking pathophysiological processes in Alzheimer's disease: an updated hypothetical model of dynamic biomarkers. *Lancet Neurology, 12*(2), 207–216. https://doi.org/10.1016/S1474-4422(12)70291-0.

Kantarci, K., Jack, C. R. Jr., Xu, Y. C., Campeau, N. G., O'Brien, P. C., Smith, G. E., …, & Petersen R.C.. (2000). Regional metabolic patterns in mild cognitive impairment and Alzheimer's disease, a 1H MRS study. *Neurology, 55*(2), 210–217.

Kantarci, K., Knopman, D. S., Dickson, D. W., Parisi, J. E., Whitwell, J. L., Weigand, S. D., …, & Jack, C. R. (2008). Alzheimer disease: Postmortem neuropathologic correlates of antemortem 1H MR spectroscopy metabolite measurements. *Radiology, 248*(1), 210–20. https://doi.org/10.1148/radiol.2481071590.

Katzman, R., Terry, R., DeTeresa, R., Brown, T., Davies, P., Fuld, P., …, & Peck, A. (1988). Clinical, pathological, and neurochemical changes in dementia: A subgroup with preserved mental status and numerous neocortical plaques. *Annals of Neurology, 23*(2), 138–144. https://doi.org/10.1002/ana.410230206.

Metastasio, A., Rinaldi, P., Tarducci, R., Mariani, E., Feliziani, F. T., Cherubini, A., …, & Mecocci, P. (2006). Conversion of MCI to dementia: role of proton magnetic resonance spectroscopy. *Neurobiology of Aging, 27*(7), 926–932. https://doi.org/10.1016/j.neurobiolaging.2005.05.002.

Minati, L., Grisoli, M., & Bruzzone, M. G. (2007). MR spectroscopy, functional MRI, and diffusion-tensor imaging in the aging brain: a conceptual review. *Journal of Geriatric Psychiatry and Neurology, 20*(1), 3–21. https://doi.org/10.1177/0891988706297089.

Modrego, P. J., Fayed, N., & Pina, M. A. (2005). Conversion from mild cognitive impairment to probable Alzheimer's disease predicted by brain magnetic resonance spectroscopy. *The American Journal of Psychiatry, 162*(4), 667–675. https://doi.org/10.1176/appi.ajp.162.4.667.

Modrego, P. J., Fayed, N., & Sarasa, M. (2011). Magnetic resonance spectroscopy in the prediction of early conversion from amnestic mild cognitive impairment to dementia: A prospective cohort study. *BMJ Open, 1*(1). https://doi.org/10.1136/bmjopen-2010-000007.

Morris, J. C. (1997). Clinical dementia rating: A reliable and valid diagnostic and staging measure for dementia of the Alzheimer type.

International Psychogeriatrics, 9(Supplement S1), 173–176. https://doi.org/10.1017/S1041610297004870.

Murray, M. E., Przybelski, S. A., Lesnick, T. G., Liesinger, A. M., Spychalla, A., Zhang, B., …, & Kantarci, K. (2014). Early Alzheimer's disease neuropathology detected by proton MR spectroscopy. *The Journal of Neuroscience: The Official Journal of the Society for Neuroscience, 34*(49), 16247–55. https://doi.org/10.1523/JNEUROSCI.2027-14.2014.

O'Neill, J., Tobias, M. C., Hudkins, M., & London, E. D. (2015). Glutamatergic neurometabolites during early abstinence from chronic methamphetamine abuse. *International Journal of Neuropsychopharmacology, 18*(3), 1–9. https://doi.org/10.1093/ijnp/pyu059.

Provencher, S. W. (2001). Automatic quantitation of localized in vivo 1H spectra with LCModel. *NMR in Biomedicine, 14*(4), 260–264. https://doi.org/10.1002/nbm.698.

Ringman, J. M., Younkin, S. G., Pratico, D., Seltzer, W., Cole, G. M., Geschwind, D. H., …, & Cummings, J. L. (2008). Biochemical markers in persons with preclinical familial Alzheimer disease. *Neurology, 71*(2), 85–92. https://doi.org/10.1212/01.wnl.0000303973.71803.81.

Ryman, D. C., Acosta-Baena, N., Aisen, P. S., Bird, T., Danek, A., Fox, N. C., …, & Bateman, R. J. (2014). Symptom onset in autosomal dominant Alzheimer disease: a systematic review and meta-analysis. *Neurology, 83*(3), 253–260. https://doi.org/10.1212/WNL.0000000000000596.

Scheltens, P., Blennow, K., Breteler, M. M. B., de Strooper, B., Frisoni, G. B., Salloway, S., Van der Flier, & aria, W. M. (2016). Alzheimer's disease. *Lancet (London, England), 388*(10043), 505–517. https://doi.org/10.1016/S0140-6736(15)01124-1.

Seese, R. R., O'Neill, J., Hudkins, M., Siddarth, P., Levitt, J., Tseng, B., …, & Caplan, R. (2011). Proton magnetic resonance spectroscopy and thought disorder in childhood schizophrenia. *Schizophrenia Research, 133*(1–3), 82–90. https://doi.org/10.1016/j.schres.2011.07.011.

Shattuck, D. W., Sandor-Leahy, S. R., Schaper, K. A., Rottenberg, D. A., & Leahy, R. M. (2001). Magnetic resonance image tissue classification using a partial volume model. *NeuroImage, 13*(5), 856–876. https://doi.org/10.1006/nimg.2000.0730.

Soares, D. P., & Law, M. (2009). Magnetic resonance spectroscopy of the brain: review of metabolites and clinical applications. *Clinical Radiology, 64*(1), 12–21. https://doi.org/10.1016/j.crad.2008.07.002.

Targosz-gajniak, M. G., Siuda, J. S., Wicher, M. M., Banasik, T. J., Bujak, M. A., Augusciak-duma, A. M., & Opala, G. (2013). Magnetic resonance spectroscopy as a predictor of conversion of mild cognitive impairment to dementia. *Journal of the Neurological Sciences, 335*(1–2), 58–63. https://doi.org/10.1016/j.jns.2013.08.023.

Wang, H., Tan, L., Wang, H. F., Liu, Y., Yin, R. H., Wang, W. Y., …, & Yu, J. T. (2015). Magnetic resonance spectroscopy in Alzheimer's disease: systematic review and meta-analysis. *Journal of Alzheimer's Disease, 46*(4), 1049–1070. https://doi.org/10.3233/JAD-143225.

Zhang, N., Song, X., Bartha, R., Beyea, S., D'Arcy, R., Zhang, Y., & Rockwood, K. (2014). Advances in high-field magnetic resonance spectroscopy in Alzheimer's disease. *Current Alzheimer Research, 2014*(11), 367–388.